

Nexus sine qua non: Essentially Connected Networks for Traffic Forecasting

Tong Nie¹, Guoyang Qin¹, Lijun Sun², Yunpeng Wang³, Jian Sun^{1*}

¹ Key Laboratory of Road and Traffic Engineering of the State Ministry of Education, Tongji University, Shanghai, China

² McGill University, Montreal, Quebec, Canada

³ School of Transportation Science and Engineering, Beihang University, Beijing, China
{nietong, 2015qgy, sunjian}@tongji.edu.cn; lijun.sun@mcgill.ca; ypwang@buaa.edu.cn

Abstract

Spatial-temporal graph neural networks (STGNNs) have become the de facto models for learning spatiotemporal representations of traffic flow. However, modern STGNNs often contain superfluous or obscure components, along with complex techniques, posing significant challenges in terms of complexity and scalability. Such concerns prompt us to rethink the design of neural architectures and to identify the key challenges in traffic forecasting as spatial-temporal contextualization. Here, we present an essentially connected model based on an efficient message-passing backbone, powered by learnable node embedding, without any complex sequential techniques such as TCNs, RNNs, and Transformers. Intriguingly, empirical results demonstrate how a simple and elegant model with contextualization capability compares favorably w.r.t. the state-of-the-art with elaborate structures, while being much more interpretable and computationally efficient for traffic forecasting. We anticipate that our findings will open new horizons for further research to explore the possibility of creating simple but effective neural forecasting architectures.

1 Introduction

Modeling and forecasting spatiotemporal traffic flow not only facilitates decision making by practitioners, but also deepens our scientific understanding of the underlying dynamic systems. Spatiotemporal traffic forecasting (STTF) is one of the most popular applications of modern neural forecasting models, and numerous works have been devoted to developing advanced spatial-temporal graph neural networks (STGNNs) that can capture complex correlations in spatiotemporal traffic data (Yu, Yin, and Zhu 2018; Li et al. 2018; Wu et al. 2019b; Bai et al. 2020; Li et al. 2023).

Stacking multiple novel spatial-temporal layers tends to be a standardized practice in newly-emerged STGNNs. Despite improvements in accuracy in common benchmarks, the introduction of complex techniques and overly cumbersome architectures hinders the understanding of their behaviors and the discovery of components that really contribute to forecasting. It is dubious that the designs of some advanced STGNNs may conceptually complicate the forecasting process. Furthermore, increasing complexity often requires extensive training time and tedious parameter tuning, making

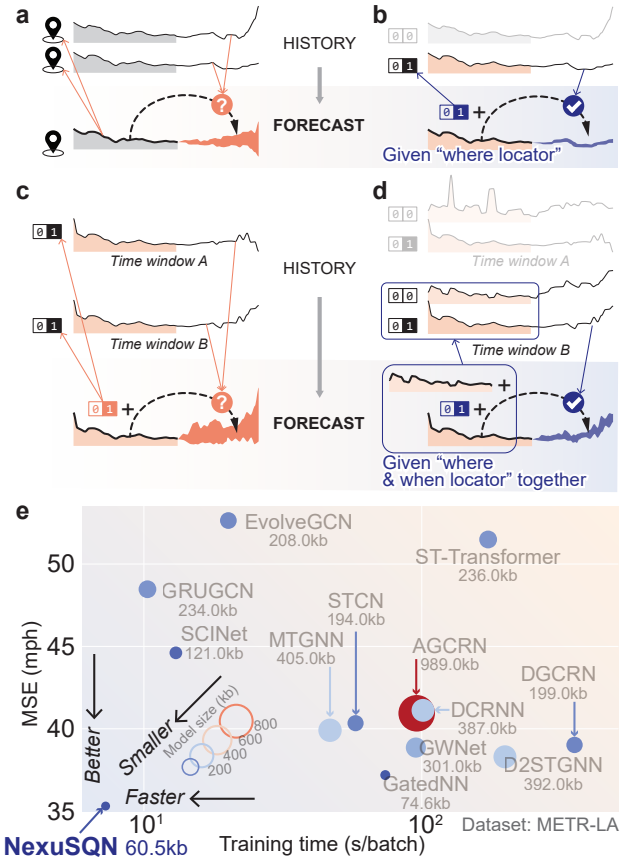


Figure 1: Illustration of the contextualization issue in spatiotemporal traffic data: (a-b) if two future series that follow identical past series are different in two different sensors, then forecasting without knowing the location becomes indistinguishable; (c-d) even at one location, if two series with identical past series are distinct at different times, the sensor identifier, since it remains constant, is no longer useful to distinguish the time-wise multivaluedness. (e) By exploiting the “where” and “when” locators, our model can achieve favorable performance in both efficacy and efficiency.

many state-of-the-art models infeasible for large-scale sensor networks (Liu et al. 2023b; Jin et al. 2023).

*Corresponding author

The above phenomena prompt us to revisit the design of STGNNs and throw out an intriguing question: **Is there an essentially simple but effective model for STTF?** With this question, we first carefully inspect the STTF task. We find the forecasting can be particularly problematic when the future series is often nondeterministic with respect to the past series within a look-back window, which means that the maps to learn are one-to-many, and a deterministic one-to-one function, however expressive it is, cannot fully capture this multivalued mapping. This is especially difficult when there is no external information available to explain away the ambiguity. A key workaround is to reconstruct *contextualization* information from the data itself to separate “many” in a higher-dimensional space and turn the multi-value mapping into a univalued mapping. By contemplating the essence of the problem, we find that it basically involves injecting two essential elements corresponding to each of the multivalued mappings, which we call a “where locator” and a “when locator”, to contextualize the forecasting task in spatial and temporal dimensions, respectively (see Fig. 1).

Using the “where locator” and “when locator” lenses, we can focus on surveying models based on how they approach the two types of contextualization in a variety of studies. We then question the necessity and validity of using complex STGNNs for STTF and argue that many of them do not alleviate the contextualization problem but make it even more difficult to distinguish spatiotemporal samples. Given the complexity and inefficiency of current models, it may be tempting to go beyond such acknowledged paradigms and explore the performance of a minimalistic model that only includes essential connection components to directly express “where locator” and “when locator”.

To achieve this, we assign a unique vector as the “where locator” for each location. However, we do not assign additional vectors as “when locator” for each piece of time, as this would increase redundant parameters. Instead, we attempt to reuse the “where locator” as learnable embeddings to correlate past series of all sensors to contextualize the temporal location of the current series. Surprisingly, in our experiments, this reuse of the “where locator” as a “when locator” can perform comparatively with its complex counterparts while enjoying much faster training, less resource consumption, and fewer model parameters (see Fig. 1(e)). Our main contributions are threefold:

- We present a conceptually simple but effective model with essentially connected components for STTF;
- We identify and highlight the significance of node embedding in spatiotemporal contextualization;
- We conduct extensive experiments to evaluate the performance of the proposed model on 7 traffic forecasting benchmarks and reveal its superiority by comparing with 15 state-of-the-art neural forecasting models.

We hope this work will incentivize further endeavor on extending beyond the sphere of complex STGNNs, and re-considering the significance of simpler models. As our goal is to identify the essential components for STTF, we name our model *Nexus Sine Qua Non* (**NexuSQN**) networks, which literally means “the connection without which, not.”

2 Notations and Preliminary

Notations and Problem Statement We investigate the multivariate traffic forecasting problem in a spatiotemporal context. For ease of representation, we follow the terminology of previous work (Cini et al. 2022). In particular, N time series are collected from different static sensors, and each of them has a d_{in} dimensional measurement of traffic flow at time t , denoted by $\mathbf{x}_t^i \in \mathbb{R}^{d_{in}}$. The entire record at time t can be linked by sensor networks and forms a graph signal matrix $\mathbf{X}_t \in \mathbb{R}^{N \times d_{in}}$ with side information represented by the static adjacent matrix (possibly time varying) $\mathbf{A} \in \mathbb{R}^{N \times N}$. In addition, we indicate with the tensor $\mathcal{X}_{t:t+T} \in \mathbb{R}^{N \times T \times d_{in}}$ the sequence of graph signals within the time interval $[t, t + T]$. For STTF dataset, exogenous variables about time stamps are readily collected for the entire period, which is denoted as $\mathbf{U}_t \in \mathbb{R}^{N \times d_s}$. Similarly, node-specific features such as sensor ids are indicated as $\mathbf{V} \in \mathbb{R}^{N \times d_v}$. Note that this paper uses the terms nodes, sensors, and locations interchangeably. Input graph signals within a time window W can be denoted as $\mathcal{G}_{T-W:T} = \langle \mathcal{X}_{T-W:T}, \{\mathbf{U}_t, \mathbf{V}, \mathbf{A}_t, t = T - W, \dots, T\} \rangle$. The objective of STTF is to forecast the next H horizons of graph signals given a length of W historical records with a predictive function $F_\theta(\cdot): \mathcal{G}_{T+1:T+H} = F_\theta(\mathcal{G}_{T-W:T} | \theta)$.

Neural Message-Passing of STGNNs GNNs can be considered as a general model of message-passing neural networks (MPNNs). MPNNs contain three forward computation phases: message passing (MP), feature aggregation, and node updating, parameterized by permutation-invariant functions (Gilmer et al. 2017). Under the spatiotemporal settings, MPNN at each time step can be formulated as follows:

$$\begin{aligned} \mathbf{m}_t^{i \leftarrow j, (l)} &= \text{MSG}_l(\mathbf{h}_t^{i, (l-1)}, \mathbf{h}_t^{j, (l-1)}, e_{i \leftarrow j}^t), \\ \mathbf{m}_t^{i, (l)} &= \text{AGG}(\mathbf{m}_t^{i \leftarrow j, (l)}; \forall j \in \mathcal{N}(i)), \\ \mathbf{h}_t^{i, (l)} &= \text{UP}_l(\mathbf{h}_t^{i, (l-1)}, \mathbf{m}_t^{i, (l)}), \end{aligned} \quad (1)$$

where $e_{i \leftarrow j}^t$ is the edge weight between node i and j at time t . An additional temporal MP process can be applied to model temporal correlations (Cini et al. 2023). Stacking several MPNNs or applying high-order ones can somewhat alleviate the spatial contextualization problem. However, these solutions are prone to the over-squashing problem (Dwivedi et al. 2022) and deficient in locating series in the time axis.

3 Essentially Connected Neural Predictors

The above discussion motivates us to develop a simple but effective model for STTF. We identify the key challenge of STTF as spatial and temporal contextualization and depend on the node embedding (NE) to learn distinguishable spatiotemporal representations. In particular, NexuSQN features an essentially connected neural architecture based on a message-passing backbone (see Fig. 2), and the rationale for NexuSQN is the versatile use of learnable node embedding and the simplicity of modular design. Notably, our model completely avoids complex temporal methods (e.g., RNNs, TCNs, and self-attention) and spatial techniques (e.g., diffusion convolutions and distance-based adjacent graphs) en-

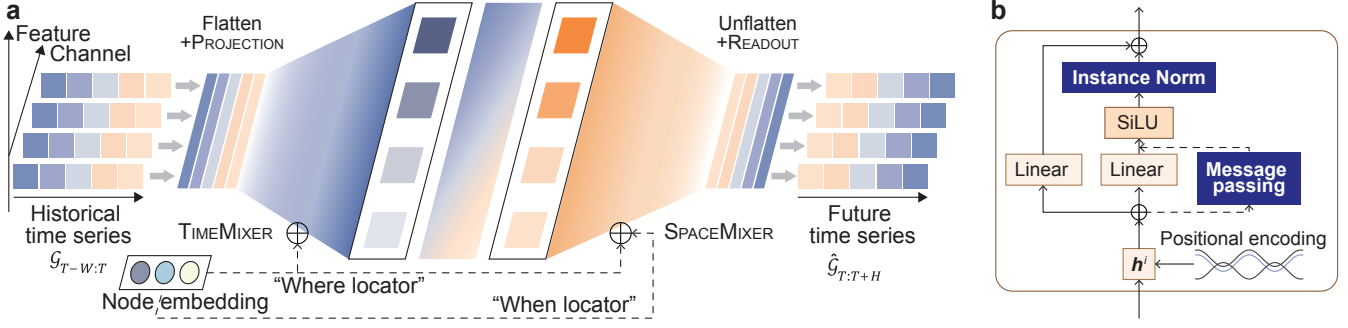


Figure 2: Architecture overview and basic block of NexuSQN. Both TIMEMIXER and SPACEMIXER follow this backbone.

tirely. With a concise and comprehensible neural predictor, we seek to empirically answer the following key questions:

- Q1** Are NE powerful for spatiotemporal contextualization?
- Q2** With NE, how to keep the model structure minimalistic?
- Q3** Are simplified model architectures effective for STTF?

With these questions, we provide detailed descriptions about each modular component in the following sections.

3.1 Overview of Architectural Components

Overview The overall architecture of NexuSQN can be concisely formulated as follows:

$$\begin{aligned}
 \mathbf{H}^0 &= \text{PROJECTION}(\mathcal{X}_{t-W:t}), \\
 \mathbf{H}^{(1)} &= \text{TIMEMIXER}(\mathbf{H}^{(0)}; \mathbf{E}_{t-W:t}), \\
 \mathbf{H}^{(l+1)} &= \text{SPACEMIXER}(\mathbf{H}^{(l)}; \mathbf{A}), \quad l \in \{1, \dots, L\} \\
 \mathcal{X}_{t:t+H} &= \text{READOUT}(\mathbf{H}^{(L+1)}),
 \end{aligned} \tag{2}$$

where TIMEMIXER and SPACEMIXER build on conceptually and technically simple MLP and MPNN blocks, which can be represented together by Fig. 2(2). \mathbf{E}_t is learnable NE, and \mathbf{A} is the relational graph. In the following paragraphs we will detail each component in turn.

Input Flattening and PROJECTION STGNNs usually handle time and feature dimension separately, i.e., first project the input features at each time step to high-dimensional representations independently and correlate different time steps with sequential models like RNNs. Despite being reasonable and intuitive, this treatment increases the model complexity and the risk of overfitting significantly, especially when the hidden dimension is much larger than the channel (feature) dimension. As such, we proposed to flatten raw time series along time dimension and project the inputs into hidden space with a simple MLP layer:

$$\begin{aligned}
 \mathbf{X}_{t-W:t} &= \text{FOLD}([\mathcal{X}_{t-W:t} \parallel \mathbf{U}_{t-W:t}], \dim = 0), \\
 \mathbf{H}^0 &= \text{MLP}(\mathbf{X}_{t-W:t}),
 \end{aligned} \tag{3}$$

where $\text{FOLD}(\cdot) : \mathbb{R}^{N \times T \times d_{in}} \rightarrow \mathbb{R}^{N \times T d_{in}}$ is the flattening operation. By flattening and projecting along the time dimension, serial information is stored in the hidden state \mathbf{H}^0 . We further inject exogenous variables \mathbf{U}_t about series properties here to inform the projection layer with time-series information, e.g., periodicity and seasonality.

TIMEMIXER for Exploiting Historical Information Time mixer models the temporal relations and patterns contained in historical series. We adopt 2-layer MLP with residual connection (He et al. 2016) to encode temporal representations:

$$\begin{aligned}
 \tilde{\mathbf{H}}^0 &= \text{SiLU}(\mathbf{H}^0 \Theta_{\text{time}}^0), \\
 \mathbf{H}^1 &= \text{IN}(\tilde{\mathbf{H}}^0) + \mathbf{H}^0 \Theta_{\text{time}}^1,
 \end{aligned} \tag{4}$$

where $\Theta_{\text{time}}^0, \Theta_{\text{time}}^1$ are linear weights, $\text{IN}(\cdot)$ is the instance normalization (Ulyanov, Vedaldi, and Lempitsky 2016), which is adopted to mitigate distribution shift (Kim et al. 2021; Nie et al. 2022) and reinforce the representations of high-frequency temporal components (Deng et al. 2021).

SPACEMIXER for Modeling Relational Information The proposed graph mixer can be viewed as a structured feature (channel) mixing layer, which is a specialization of the vanilla MLP mixer (Chen et al. 2023). As shown in Fig. 2, what differentiates SPACEMIXER from TIMEMIXER is the MP step that aggregates neighborhood features on graphs.

Considering the dependence of channels (sensors), the MLP mixer can be formulate as:

$$\mathbf{H}^{(l)} = \sigma(\Theta_{\text{channel}}^{(l)} \mathbf{H}^{(l-1)} \Theta_{\text{time}}^{(l)}), \tag{5}$$

where Θ_{feature} is the channel mixing weight and can also be interpreted as an unconstrained graph learning module that contains N^2 parameters. To specialize this model, we adopt a structured MPNN as the featured block of graph mixer:

$$\text{MPNN}^{(l)}(\mathbf{H}^{(l-1)}; \mathbf{A} | \Theta) = \text{SiLU}(\mathbf{A} \mathbf{H}^{(l-1)} \Theta_{\text{time}}^{(l)}), \tag{6}$$

where \mathbf{A} is the relational graphs, which can be either a priori ones or adaptively learned. It can be seen that our space mixer exploits the characteristics of adjacent matrices and explicitly models the pairwise interactions among nodes. By seizing relational information, our model achieves a modular extension from univariate models to multivariate.

Dense READOUT For multi-step STTF, we adopt a MLP and reshaping layer to directly output the predictions:

$$\begin{aligned}
 \hat{\mathbf{X}}_{t:t+H} &= \text{MLP}(\mathbf{H}^{(L)}), \\
 \hat{\mathcal{X}}_{t:t+H} &= \text{UNFOLD}(\hat{\mathbf{X}}_{t:t+H}),
 \end{aligned} \tag{7}$$

where $\text{UNFOLD}(\cdot)$ is the inverse linear operator of $\text{FOLD}(\cdot)$. Again, we do not elaborate on a complex sequential decoder, and the multistep predictions are regressed directly.

3.2 Node Embedding for When-Where Contextualization

One cornerstone of the proposed framework is the versatility of NE. To tackle the spatial-temporal contextualization issue, the roles of NE in our model are twofold, including: *where locator* and *when locator*, which correspond to positional and structural representation in the theory of GNNs’ representation learning (Srinivasan and Ribeiro 2019).

Spatial-Temporal Node Embedding For the space dimension, we consider setting a unique identifier for each sensor. An optional structural embedding is the random-walk diffusion matrix (Dwivedi et al. 2020). For simplicity, we use the learnable NE as a simple index positional encoding without any structural priors. As for implementation, we assign a learnable vector of size d_{emb} with random initialization for each series, denoted as $\mathbf{E} \in \mathbb{R}^{N \times d_{\text{emb}}}$, then \mathbf{E} is included in the forward computation as endogenous variables and its gradient is updated end-to-end by backpropagation.

This NE reflects the static features of each sensor, e.g., dominating traffic patterns (Nie et al. 2023a), and is agnostic to temporal information. Inspired by (Marisca, Cini, and Alippi 2022), we propose to inform the model with stationary serial property of traffic flows, e.g., periodicity and seasonality. The sinusoidal positional encoding (Vaswani et al. 2017) $\mathbf{U}_t \in \mathbb{R}^{T \times d_s}$ is adopted to inject the time-of-day information to all series. Given \mathbf{U}_t , we first fold the time dimension and project it into the hidden space:

$$\begin{aligned} \tilde{\mathbf{u}} &= \mathbf{W}_U \text{FOLD}(\mathbf{U}_t), \\ \tilde{\mathbf{U}} &= \text{BROADCAST}(\tilde{\mathbf{u}}, N), \\ \mathbf{E}_t &= \text{RESMLP}(\text{RESMLP}(\mathbf{E} + \tilde{\mathbf{U}})), \end{aligned} \quad (8)$$

where $\mathbf{W}_U \in \mathbb{R}^{d_{\text{emb}} \times T d_s}$ is learnable weights, and $\text{BROADCAST}(\cdot)$ duplicates the inputs with given times along a new dimension. \mathbf{E}_t is the final spatiotemporal node embedding (STNE). Since input data from different time-of-day intervals has different sinusoidal stamps, STNE can reflect periodicity of series. The following paragraphs explain how this STNE contributes to the traffic forecasting process.

“Where Locator” It can be seen that Eqs. 4 and 6 are global models shared by all sensors. Given two sensors with similar historical inputs, such global models fail to contextualize each series in the spatial dimension, even though they have different dynamics in the future. To circumvent such a one-to-many problem, we parameterize each node with a discriminative identifier using the STNE. Especially, we add the learnable \mathbf{E}_t to each series in the first MLP of TIMEMIXER as spatial contextualization directly:

$$\tilde{\mathbf{h}}_i^0 = \text{MLP}(\mathbf{h}_i^0 + \mathbf{e}_i). \quad (9)$$

Notably, the introduction of learnable embedding in each node is shown to be equivalent to the specialization of the univariate model (Cini et al. 2023), which benefits the use of node-specific local dynamics (Sen, Yu, and Dhillon 2019).

On the other hand, since GNNs focus on local graph structures, they are inadequate to distinguish between two nodes with close neighborhood structure, which is understood as

a spatial indistinguishability problem (Dwivedi et al. 2022). Therefore, to allow the aggregation function to be aware of the difference of each node, so that the node features can still be discriminated after the message aggregation, we include \mathbf{E}_t in the MP process in Eq. 1:

$$\mathbf{m}_t^{i \leftarrow j} = \text{MSG} \left(\begin{bmatrix} \mathbf{h}_t^i \\ \mathbf{e}^i \end{bmatrix}, \begin{bmatrix} \mathbf{h}_t^j \\ \mathbf{e}^j \end{bmatrix}, a_{i \leftarrow j}^t \right). \quad (10)$$

We claim that adding learnable features to the message function is equivalent to incorporating high-frequency components into low-frequency representations to highlight the impact of local events in spatiotemporal data. Actually, the random node initialization itself enhances the GNNs (Sato, Yamada, and Kashima 2021). As can be seen, the “where locator” only implies the exclusivity of the identifier, we set it to be learnable for the sake of reuse for the “when locator”.

“When Locator” STNE represents the dominant traffic flow patterns and can be understood as a global and static identifier. If a sensor’s readings are different at two different times but share a close historical series, the “where locator” alone is less effective at contextualizing its temporal information. In this case, an additional “when locator” is needed.

Following the discussions in (Chen et al. 2023), we can first divide forecasting models into two categories according to their encoding mechanisms: (1) time-dependent and (2) data-dependent. Concretely, a linear predictive model with weight \mathbf{W} and bias \mathbf{b} can be expressed as:

$$\begin{aligned} \mathbf{x}_{t+1:t+H} &= \mathbf{W} \mathbf{x}_{t-W:t} + \mathbf{b}, \\ \text{or: } x_{t+h} &= \sum_{k=0}^W w_{k,h} x_{t-k} + b_{k,h}, \quad h \in \{1, \dots, H\}, \end{aligned} \quad (11)$$

which forms a vanilla autoregressive (AR) model at each forecast horizon, where the AR parameters depend only on the relative order and are agnostic to the location in the historical sequence. The TIMEMIXER works in this way.

One natural “when locator” for time-dependent model is to assign a unique identifier to each piece of time. However, there exists three drawbacks: (1) since the prediction is basically done sequence-to-sequence, having different identifiers within a time window is redundant; (2) the time-dependent model in Eq. 11 relies on relative timestamps and the use of absolute ones is difficult for it; (3) timestamp-based encoding would attribute the ambiguity to time-varying factors, e.g., rush hour, but this may be caused by local high-frequency spatial dynamics such as the spread of traffic congestion or irregular driving behavior.

Conversely, the behaviors of data-dependent models are pattern-aware and condition on local temporal variations:

$$x_{t+h} = \sum_{k=0}^W \mathcal{F}_k(\mathbf{x}_{t-W:t}) x_{t-k} + b_{k,h}, \quad h \in \{1, \dots, H\}, \quad (12)$$

where $\mathcal{F}_k(\cdot)$ is a data-driven function, e.g., self-attention. We argue that this forms a fully time-varying AR model (Bringmann et al. 2017) in which the AR process is parameterized by time-varying coefficients. This overparameterization tends to overfit the data rather than capture the temporal relationships such as the location on the time axis.

Given that the series of adjacent nodes within a specified period exhibits significant temporal dynamics, it can itself be used as a “when locator”. With this in mind, we propose to reuse “where locator” as a query for all available reference series to contextualize the temporal patterns. In essence, we only need to specify the relation graphs in Eq. 6:

$$\mathbf{A}_t = \text{SOFTMAX}(\mathbf{E}_t \cdot \mathbf{E}_t^T). \quad (13)$$

Since \mathbf{E}_t is aware of the time-of-day feature, this query function is time-varying within a period. Our approach lies between the time-dependent and data-dependent routines and can forecast with both relative time stamp and local spatial patterns. In this way, the positional node embeddings and structural graph representations are equivalently unified (Srinivasan and Ribeiro 2019) in spatiotemporal graphs.

3.3 Remarks on Parameter-Efficient Neural Message-Passing Designs

Another ingenuity of NexuSQN is its parameter-efficient MP backbone. We present several task-agnostic techniques to lighten the overall neural architecture. Note that since NexuSQN propagates features only after the temporal encoder, rather than at every time step, it is more efficient than alternately stacked spatial-temporal blocks.

Residual Connection We keep a shortcut for the linear part in each block. When all residual connections are activated (e.g., when graph relation is unnecessary), our model can degenerate into a class of linear models with channel-independence, e.g., (Zeng et al. 2022; Das et al. 2023), which show great potential for long-term series forecasting.

Parameter Sharing Different from recent design trends that assign different node parameters or graphs for different layers (Zhang et al. 2020; Oreshkin et al. 2021), we set the NE globally shared for all modules. The idea is to facilitate end-to-end training of random node features and reduction of model size. In addition, recent works empirically show that MLPs and MPNNs can share similar feature spaces (Yang et al. 2022; Han et al. 2022). Without MP, SPACEMIXER can collapse into TIMEMIXER. Considering this, we instantiate the successive MP layers with a common linear transform for time mixing.

Shallow-Layer Structure Instead of multilayer deep GNN structures, we adopt shallow-layer structures with larger receptive field. In particular, we consider using one or two layers of MPNN with fully connected graphs to capture long-range spatial dependence, without multiple stacked sparse graph aggregators or hierarchical operations, e.g., diffusion graph convolutions (Li et al. 2018). Recent studies reveal that the expressive power of GNNs are determined by both of the depth and width (Loukas 2019), and wider GNNs can be more expressive than deeper ones (Wu et al. 2019a). A single MP can gather adequate information from a large number of nodes when the underlying graph is dense.

4 Related Works

Spatiotemporal traffic forecasting has sparked great interest in both academia and industry. As a standard paradigm,

STGNNs take all series as input and use GNNs to correlate them. The properties of traffic flow series are preserved by an elaborate sequential model. Remarkable results have been achieved in a variety of studies using STGNNs (Yu, Yin, and Zhu 2018; Li et al. 2018; Wu et al. 2019b; Bai et al. 2020; Guo et al. 2019; Zheng et al. 2020). However, modern STGNNs tend to be complex and nontrivial to implement.

Research on simplified deep models for STTF has been relatively limited. Cini et al. (2022) propose a scalable STGNN based on preprocessing that encodes spatiotemporal features prior to training. Liu et al. (2023a) replace the GNNs with feature aggregation and use a graph sampling strategy. While, both of them rely on complex temporal encoders and pre-computed graph features. Similarly to our work, Satorras, Rangapuram, and Januschowski (2022) developed a fully connected gated GNN model (GatedGN) using a graph inference structure. However, all pairwise attention is computationally very expensive. Along another path of research, several methods have emerged to challenge the existing complex models for LTSF, e.g., LightTS (Zhang et al. 2022), LTSF-Linear (Zeng et al. 2022), TS-Mixer (Chen et al. 2023) and TiDE (Das et al. 2023). While most adopt a channel-independence assumption and do not include explicit relational modeling.

Regarding positional encoding in STGNNs, Shao et al. (2022a) applies learnable embedding to all nodes, time of day, and day of week points, enabling MLPs to achieve competitive performance on multiple datasets. However, over-parameterized identifiers would be redundant and prone to overfit. Additionally, this kind of temporal identifier only reflect time-varying components and is less effective in capturing local nonstationary spatial dynamics. Cini et al. (2023) further interpreted the role of node embedding as local effects and incorporated it into a global-local architecture.

In summary, none of the existing works has directly and thoroughly investigated the essential model components for spatiotemporal traffic forecasting, nor provided exhaustive discussions on the contextualization issue in STGNNs.

5 Empirical Evaluation

Extensive experiments are carried out to evaluate the performance of the NexuSQN model on 7 well-known traffic forecasting benchmarks and compare it with 15 neural forecasting baselines. Details about experimental settings are provided in the Appendix. **PyTorch implementations and reproducible results are publicly available [code]**¹.

5.1 Experiment Setup

Datasets Six high resolution traffic flow datasets are used to compare short-term forecast performance, including two traffic speed data: METR-LA and PEMS-BAY datasets (Li et al. 2018), and four traffic volume data (Guo et al. 2021): PEMS03, PEMS04, PEMS07, and PEMS08. All these traffic measurements are obtained from loop sensors installed on highway networks and aggregated at 5 min. In particular, the six datasets provide adjacent matrices constructed by the pairwise geographic distance between sensors. The same

¹Code will be open-sourced upon publication.

DATASET	METR-LA						PEMS-BAY						PEMS03					
	15 min	30 min	60 min	Average			15 min	30 min	60 min	Average			15 min	30 min	60 min	Average		
	MAE	MAE	MAE	MAE	MSE	MAPE (%)	MAE	MAE	MAE	MAE	MSE	MAPE (%)	MAE	MAE	MAE	MAE	MAPE (%)	
AGCRN	2.85	3.19	3.56	3.14	40.94	8.69	1.38	1.69	1.94	1.63	13.59	3.71	14.65	15.72	16.82	15.58	15.08	
DCRNN	2.81	3.23	3.75	3.20	41.12	8.90	1.37	1.72	2.09	1.67	14.52	3.78	14.59	15.76	18.18	15.90	15.74	
GWNet	2.74	3.14	3.58	3.09	38.86	8.52	1.31	1.65	1.96	1.59	13.31	3.57	13.67	14.60	16.23	14.66	14.88	
GatedGN	2.72	3.05	3.43	3.01	37.19	8.20	1.34	1.65	1.92	1.58	13.17	3.55	13.72	15.49	19.08	17.08	14.44	
GRUGCN	2.93	3.47	4.24	3.46	48.47	9.85	1.39	1.81	2.30	1.77	16.70	4.03	14.63	16.44	19.87	16.62	15.96	
EvolveGCN	3.27	3.82	4.59	3.81	52.64	10.56	1.53	2.00	2.53	1.95	18.98	4.43	17.07	19.03	22.22	19.11	18.61	
ST-Transformer	2.97	3.53	4.34	3.52	51.49	10.06	1.39	1.81	2.29	1.77	17.01	4.09	14.03	15.72	18.74	15.85	15.37	
STCN	2.84	3.25	3.80	3.23	40.34	9.02	1.37	1.71	2.08	1.66	14.11	3.75	14.27	15.49	18.02	15.61	16.07	
STID	2.82	3.18	3.56	3.13	41.83	9.07	1.32	1.64	1.93	1.58	13.05	3.58	13.88	15.26	17.41	15.27	16.39	
MTGNN	2.79	3.12	3.46	3.07	39.91	8.57	1.34	1.65	1.91	1.58	13.52	3.51	13.74	14.76	16.13	14.70	14.90	
D2STGNN	2.74	3.08	3.47	3.05	38.30	8.44	1.30	1.60	1.89	1.55	12.94	3.50	13.36	14.45	15.96	14.45	14.55	
DGCRN	2.73	3.10	3.54	3.07	39.02	8.39	1.33	1.65	1.95	1.59	13.12	3.61	13.83	14.77	16.14	14.73	14.86	
SCINet	3.06	3.47	4.09	3.47	44.61	9.93	1.52	1.85	2.24	1.82	14.92	4.14	14.39	15.25	17.37	15.43	15.37	
NexuSQN	2.65	2.99	3.37	2.95	35.10	8.05	1.30	1.60	1.86	1.53	12.22	3.42	13.26	14.27	15.82	14.25	14.12	

DATASET	PEMS04					PEMS07					PEMS08				
	15 min	30 min	60 min	Average		15 min	30 min	60 min	Average		15 min	30 min	60 min	Average	
	MAE	MAE	MAE	MAE	MAPE (%)	MAE	MAE	MAE	MAE	MAPE (%)	MAE	MAE	MAE	MAE	MAPE (%)
AGCRN	18.27	18.95	19.83	18.90	12.69	19.55	20.65	22.40	20.64	9.42	14.50	15.16	16.41	15.23	10.46
DCRNN	19.19	20.54	23.55	20.75	14.32	20.47	22.11	25.77	22.30	9.51	14.84	15.93	18.22	16.06	10.40
GWNet	18.17	18.96	20.23	18.95	13.59	19.87	20.97	23.53	21.13	9.96	14.21	14.99	16.45	15.02	9.70
GatedGN	18.10	18.84	20.03	18.81	13.11	21.01	22.74	25.81	22.68	10.18	14.07	14.96	16.27	14.91	9.64
GRUGCN	19.89	22.28	27.37	22.68	15.81	21.15	24.00	29.91	24.37	10.29	15.46	17.32	21.16	17.55	11.43
EvolveGCN	23.21	25.82	30.97	26.21	17.79	24.72	28.09	34.41	28.40	12.11	18.21	20.46	24.45	20.64	13.11
ST-Transformer	19.13	21.33	25.69	21.63	15.12	20.17	22.80	27.74	23.05	9.77	14.39	15.87	18.69	16.00	10.71
STCN	19.26	20.75	24.03	20.95	14.79	20.26	22.33	26.58	22.53	9.66	14.81	16.02	18.76	16.20	10.57
STID	17.77	18.60	20.01	18.60	12.87	18.66	19.93	21.91	19.88	8.82	13.53	14.29	15.75	14.32	9.69
MTGNN	17.88	18.49	19.62	18.48	12.76	18.94	20.23	22.23	20.19	8.59	13.80	14.57	15.82	14.57	9.46
D2STGNN	17.60	18.39	19.63	18.39	12.65	-	-	-	-	-	13.65	14.53	16.00	14.52	9.40
DGCRN	18.05	18.76	20.07	18.77	13.13	-	-	-	-	-	13.96	14.68	15.96	14.70	9.62
SCINet	18.30	19.03	20.85	19.19	13.31	21.63	22.89	25.96	23.11	10.00	14.57	15.60	17.75	15.77	10.13
NexuSQN	17.48	18.20	19.37	18.19	12.58	18.48	19.71	21.63	19.68	8.25	13.38	14.19	15.50	14.20	9.26

- Best results are bold marked. Note that - indicates the model runs out of memory with the minimum batch size.

Table 1: Results on METR-LA, PEMS-BAY, PEMS03, PEMS04, PEMS07, and PEMS08 datasets. MAE for 15, 30, 60 minutes forecasting horizons, as well as MAE, MSE, and MAPE averaged over a one hour (12 steps) are reported.

graphs from previous work (Wu et al. 2019b; Marisca, Cini, and Alippi 2022) are prepared for baselines that require pre-defined graphs. Then we evaluate the scalability and the ability to forecast long-term series on the TrafficL benchmark (Lai et al. 2018), which provides records of hourly road occupancy rates measured by 862 sensors for 48 months on San Francisco Bay Area freeways.

Baselines We consider a variety of deep learning baselines in the literature to benchmark our model: AGCRN (Bai et al. 2020); DCRNN (Li et al. 2018); GWNet (Wu et al. 2019b); GatedGN (Satorras, Rangapuram, and Januschowski 2022); GRUGCN (Gao and Ribeiro 2022); EvolveGCN (Pareja et al. 2020); ST-Transformer (Xu et al. 2020); STCN (Yu, Yin, and Zhu 2018); STID (Shao et al. 2022a); MTGNN (Wu et al. 2020); D2STGNN (Shao et al. 2022b); SCINet (Liu et al. 2022); DGCRN (Li et al. 2022); DLinear (Zeng et al. 2022); TimesNet (Wu et al. 2022). To give a fair comparison, we use the official implementations in their original papers and use the recommended hyper-parameters on each dataset as far as possible. All baselines are evaluated under the same training, validation, and testing environments.

Experimental Setups We follow the same experiment setups as used in previous works whatever possible to provide unbiased evaluations. For six short-term datasets, we use 12-step historical series (1 hour) to forecast future 12-step observations. For large-scale TrafficL data, we adopt the settings in (Wu et al. 2022) that 96 steps are used as input and predictions at next {96, 192, 288, 384} steps are used for

evaluation. Quantitative metrics including mean absolute error (MAE), mean squared error (MSE), and mean absolute percentage error (MAPE) are calculated.

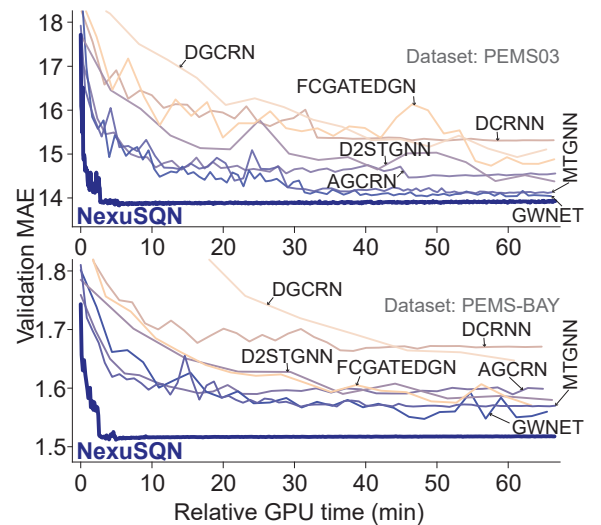


Figure 3: Validation MAE curves of different models.

5.2 Results

Short-term Traffic Benchmarks Model comparison results on six short-term speed and volume benchmarks are

given in the Tab. 1. Intriguingly, NexuSQN has achieved performances comparable to or better than its other complicated counterparts. In particular, forecasting METR-LA data is supposed to be more challenging due to complex temporal patterns, while our model consistently outperforms baselines by a large margin, even without popular sequential techniques (Q3). For PEMS-BAY data, NexuSQN is still among the best-performing predictors. Compared to STID, our model features the extraction of distinguishable low-frequency node representations with more effective “when locators”, thus showing better accuracy in all scenarios. Additionally, attention-based methods such as GatedGN, MT-GNN, and D2STGNN also show competitive results. However, high memory consumption and computational complexity hinder them from large-scale applications.

Similar observations can be made in the traffic volume datasets. Although NexuSQN does not depend on a predefined adjacent matrix, it still achieves SOTA performance. Unlike the loop speed, distance-based correlation metrics may fail to describe the behavior of traffic volumes (Nie et al. 2023b). Our observation further confirms this claim. It is worth commenting that PeMS07 contains more than eight hundred sensors, so that the attention mechanism on the spatial dimension will lead to a prohibitive memory cost. Finally, with spatiotemporal contextualization, NexuSQN can take advantage of relational information to improve forecasting with a simple structure (Q1).

	METR-LA				PEMS-BAY			
	Speed (Batch/s)	Memory (GB)	Batch size	Model size (k)	Speed (Batch/s)	Memory (GB)	Batch size	Model size (k)
AGCRN	10.43	4.1	64	989	6.78	6.0	64	991
DCRNN	9.90	3.8	64	387	6.72	5.5	64	387
GWNet	10.50	3.4	64	301	7.11	5.0	64	303
GatedGN	13.53	6.0	32	74.6	11.27	7.1	16	82.2
STCN	17.31	2.9	64	194	12.05	3.8	64	194
MTGNN	21.39	2.9	64	405	13.54	4.9	64	573
D2STGNN	5.02	6.9	32	392	5.38	7.0	16	394
DGCRN	2.82	8.0	64	199	2.74	6.9	32	208
SCINet	76.72	2.6	64	121	78.12	2.7	64	316
NexuSQN	137.35	1.2	64	60.5	90.26	1.3	64	75.6

Table 2: Model computational performances.

Computational Performance Apart from results on forecasting precision, we also examine the computational performance. Fig. 3 displays the validation MAE curves of several competing STGNNs on two datasets. Detailed records of training speed, model size and memory usage on METR-LA are exemplified in Tab. 2. Notably, NexuSQN enjoys a much faster training speed (converge in ten minutes of GPU time), smoother convergence curve, lower error bound, and less training expense, indicating high efficiency and scalability. This superiority is achieved through a technically simple structure, node embedding reuse, and parameter-efficient backbones (Q2). Advanced STGNNs like DGCRN, D2STGNN apply a series of alternating graph convolution and temporal models, resulting in a high computational burden and unstable optimization. Extra operations such as self-attention or graph attention further complicate the process.

	Models	NexuSQN	DLinear	TimesNet	SCINet
	Metric	MAE ($\times 10^{-2}$)	MAE	MAE	MAE
TrafficL	96	1.206	1.299	1.312	1.207
	192	1.273	1.407	1.411	1.398
	288	1.280	1.739	1.434	1.410
	384	1.345	1.921	1.521	1.471
Ave.	NMAE	1.752	2.144	1.883	1.855
	MRE (%)	21.03	25.73	22.60	22.27
	MAPE (%)	41.03	46.22	44.87	50.33

- We do not use normalization on the raw data and report the original metrics.

Table 3: Long-term horizon forecasting results.

Long-term Forecasting Performances We also examine the ability to predict long-term series. Tab. 3 reports the results of different prediction horizons with a 96-step sequence as input. Compared to three strong baselines in the LTSF literature, NexuSQN shows great potential to handle the challenging LTSF task. This may be because our model can encode series with both relative time stamp and local patterns.

Variations	METR-LA			PEMS03		
	w/o E	w A_{pre}	w S_{emb}	w/o E	w A_{pre}	w S_{emb}
Metric	MAE	MAE	MAE	MAE	MAE	MAE
15 min	2.88	2.64	2.84	14.85	13.48	14.64
30 min	3.32	2.98	3.23	16.62	14.54	15.91
60 min	3.76	3.38	3.65	18.68	15.95	17.45
Ave.	MAE	3.25	2.95	3.18	16.46	14.45
	MSE	39.97	35.89	39.40	766.64	610.47

Table 4: Ablation studies on METR-LA and PEMS03 data.

Ablation Study We conduct ablation studies to test the rationality of model designs. Tab. 4 reports the forecasting performance of different model variations: w/o E indicates the node embedding is removed and NexuSQN degrades into a MLP-mixer; w A_{pre} incorporates the predefined graphs with additional diffusion graph convolution (Li et al. 2018); w S_{emb} means that we replace the STNE with timestamp-based embedding. The results clearly confirm the essence of the model designs and corroborate our hypothesis (Q1, Q2).

6 Conclusion and Outlook

This work goes beyond the realm of typical STGNNs and demonstrates an essentially connected network NexuSQN for traffic forecasting. We identify the core challenge of STTF as spatial-temporal contextualization and design “where” and “when” locators to tackle it. NexuSQN features a simple structure and a parameter-efficient backbone. Extensive and rigorous evaluations on several benchmarks indicate that NexuSQN not only outperforms a diverse array of baselines but also enjoys high computational efficiency. We believe that NexuSQN will form the basis for further research on understanding and designing simpler neural forecasting models and will help practitioners develop more efficient tools in industrial applications. Future work includes further exploration of performance on larger-scale datasets and a wider variety of data, as well as the interpretability.

Acknowledgments

This research was sponsored by the National Natural Science Foundation of China (52125208), and the Science and Technology Commission of Shanghai Municipality (No. 22dz1203200).

References

- Bai, L.; Yao, L.; Li, C.; Wang, X.; and Wang, C. 2020. Adaptive graph convolutional recurrent network for traffic forecasting. *Advances in neural information processing systems*, 33: 17804–17815.
- Bringmann, L. F.; Hamaker, E. L.; Vigo, D. E.; Aubert, A.; Borsboom, D.; and Tuerlinckx, F. 2017. Changing dynamics: Time-varying autoregressive models using generalized additive modeling. *Psychological methods*, 22(3): 409.
- Chen, C.; Petty, K.; Skabardonis, A.; Varaiya, P.; and Jia, Z. 2001. Freeway performance measurement system: mining loop detector data. *Transportation Research Record*, 1748(1): 96–102.
- Chen, S.-A.; Li, C.-L.; Yoder, N.; Arik, S. O.; and Pfister, T. 2023. Tsmixer: An all-mlp architecture for time series forecasting. *arXiv preprint arXiv:2303.06053*.
- Cini, A.; and Marisca, I. 2022. Torch Spatiotemporal.
- Cini, A.; Marisca, I.; Bianchi, F. M.; and Alippi, C. 2022. Scalable Spatiotemporal Graph Neural Networks. *arXiv preprint arXiv:2209.06520*.
- Cini, A.; Marisca, I.; Zambon, D.; and Alippi, C. 2023. Taming Local Effects in Graph-based Spatiotemporal Forecasting. *arXiv preprint arXiv:2302.04071*.
- Das, A.; Kong, W.; Leach, A.; Sen, R.; and Yu, R. 2023. Long-term Forecasting with TiDE: Time-series Dense Encoder. *arXiv preprint arXiv:2304.08424*.
- Deng, J.; Chen, X.; Jiang, R.; Song, X.; and Tsang, I. W. 2021. St-norm: Spatial and temporal normalization for multi-variate time series forecasting. In *Proceedings of the 27th ACM SIGKDD conference on knowledge discovery & data mining*, 269–278.
- Dwivedi, V. P.; Joshi, C. K.; Luu, A. T.; Laurent, T.; Bengio, Y.; and Bresson, X. 2020. Benchmarking graph neural networks. *arXiv preprint arXiv:2003.00982*.
- Dwivedi, V. P.; Luu, A. T.; Laurent, T.; Bengio, Y.; and Bresson, X. 2022. Graph Neural Networks with Learnable Structural and Positional Representations. In *International Conference on Learning Representations*.
- Gao, J.; and Ribeiro, B. 2022. On the Equivalence Between Temporal and Static Equivariant Graph Representations. In *International Conference on Machine Learning*, 7052–7076. PMLR.
- Gilmer, J.; Schoenholz, S. S.; Riley, P. F.; Vinyals, O.; and Dahl, G. E. 2017. Neural message passing for quantum chemistry. In *International Conference on Machine Learning*, 1263–1272. PMLR.
- Guo, S.; Lin, Y.; Feng, N.; Song, C.; and Wan, H. 2019. Attention based spatial-temporal graph convolutional networks for traffic flow forecasting. In *Proceedings of the AAAI Conference on Artificial Intelligence*, volume 33, 922–929.
- Guo, S.; Lin, Y.; Wan, H.; Li, X.; and Cong, G. 2021. Learning dynamics and heterogeneity of spatial-temporal graph data for traffic forecasting. *IEEE Transactions on Knowledge and Data Engineering*, 34(11): 5415–5428.
- Han, X.; Zhao, T.; Liu, Y.; Hu, X.; and Shah, N. 2022. MLPInit: Embarrassingly Simple GNN Training Acceleration with MLP Initialization. *arXiv preprint arXiv:2210.00102*.
- He, K.; Zhang, X.; Ren, S.; and Sun, J. 2016. Deep residual learning for image recognition. In *Proceedings of the IEEE conference on computer vision and pattern recognition*, 770–778.
- Hummon, M.; Ibanez, E.; Brinkman, G.; and Lew, D. 2012. Sub-hour solar data for power system modeling from static spatial variability analysis. Technical report, National Renewable Energy Lab.(NREL), Golden, CO (United States).
- Jin, M.; Koh, H. Y.; Wen, Q.; Zambon, D.; Alippi, C.; Webb, G. I.; King, I.; and Pan, S. 2023. A Survey on Graph Neural Networks for Time Series: Forecasting, Classification, Imputation, and Anomaly Detection. *arXiv preprint arXiv:2307.03759*.
- Kim, T.; Kim, J.; Tae, Y.; Park, C.; Choi, J.-H.; and Choo, J. 2021. Reversible instance normalization for accurate time-series forecasting against distribution shift. In *International Conference on Learning Representations*.
- Lai, G.; Chang, W.-C.; Yang, Y.; and Liu, H. 2018. Modeling long-and short-term temporal patterns with deep neural networks. In *The 41st international ACM SIGIR conference on research & development in information retrieval*, 95–104.
- Li, F.; Feng, J.; Yan, H.; Jin, G.; Yang, F.; Sun, F.; Jin, D.; and Li, Y. 2023. Dynamic graph convolutional recurrent network for traffic prediction: Benchmark and solution. *ACM Transactions on Knowledge Discovery from Data*, 17(1): 1–21.
- Li, Y.; Yu, R.; Shahabi, C.; and Liu, Y. 2018. Diffusion Convolutional Recurrent Neural Network: Data-Driven Traffic Forecasting. In *International Conference on Learning Representations*.
- Liu, M.; Zeng, A.; Chen, M.; Xu, Z.; Lai, Q.; Ma, L.; and Xu, Q. 2022. Scinet: Time series modeling and forecasting with sample convolution and interaction. *Advances in Neural Information Processing Systems*, 35: 5816–5828.
- Liu, X.; Liang, Y.; Huang, C.; Hu, H.; Cao, Y.; Hooi, B.; and Zimmermann, R. 2023a. Do We Really Need Graph Neural Networks for Traffic Forecasting? *arXiv preprint arXiv:2301.12603*.
- Liu, X.; Xia, Y.; Liang, Y.; Hu, J.; Wang, Y.; Bai, L.; Huang, C.; Liu, Z.; Hooi, B.; and Zimmermann, R. 2023b. LargeST: A Benchmark Dataset for Large-Scale Traffic Forecasting. *arXiv preprint arXiv:2306.08259*.
- Loukas, A. 2019. What graph neural networks cannot learn: depth vs width. *arXiv preprint arXiv:1907.03199*.
- Marisca, I.; Cini, A.; and Alippi, C. 2022. Learning to Reconstruct Missing Data from Spatiotemporal Graphs with Sparse Observations. *arXiv preprint arXiv:2205.13479*.

- Nie, T.; Qin, G.; Wang, Y.; and Sun, J. 2023a. Correlating sparse sensing for large-scale traffic speed estimation: A Laplacian-enhanced low-rank tensor kriging approach. *Transportation Research Part C: Emerging Technologies*, 152: 104190.
- Nie, T.; Qin, G.; Wang, Y.; and Sun, J. 2023b. Towards better traffic volume estimation: Tackling both underdetermined and non-equilibrium problems via a correlation adaptive graph convolution network. *arXiv preprint arXiv:2303.05660*.
- Nie, Y.; Nguyen, N. H.; Sinthong, P.; and Kalagnanam, J. 2022. A Time Series is Worth 64 Words: Long-term Forecasting with Transformers. *arXiv preprint arXiv:2211.14730*.
- Oreshkin, B. N.; Amini, A.; Coyle, L.; and Coates, M. 2021. FC-GAGA: Fully connected gated graph architecture for spatio-temporal traffic forecasting. In *Proceedings of the AAAI Conference on Artificial Intelligence*, volume 35, 9233–9241.
- Pareja, A.; Domeniconi, G.; Chen, J.; Ma, T.; Suzumura, T.; Kanezashi, H.; Kaler, T.; Schardl, T.; and Leiserson, C. 2020. Evolvegcn: Evolving graph convolutional networks for dynamic graphs. In *Proceedings of the AAAI conference on artificial intelligence*, volume 34, 5363–5370.
- Paszke, A.; Gross, S.; Massa, F.; Lerer, A.; Bradbury, J.; Chanan, G.; Killeen, T.; Lin, Z.; Gimelshein, N.; Antiga, L.; et al. 2019. Pytorch: An imperative style, high-performance deep learning library. *Advances in neural information processing systems*, 32: 8026–8037.
- Sato, R.; Yamada, M.; and Kashima, H. 2021. Random features strengthen graph neural networks. In *Proceedings of the 2021 SIAM International Conference on Data Mining (SDM)*, 333–341. SIAM.
- Satorras, V. G.; Rangapuram, S. S.; and Januschowski, T. 2022. Multivariate Time Series Forecasting with Latent Graph Inference. *arXiv preprint arXiv:2203.03423*.
- Sen, R.; Yu, H.-F.; and Dhillon, I. S. 2019. Think globally, act locally: A deep neural network approach to high-dimensional time series forecasting. *Advances in neural information processing systems*, 32.
- Shao, Z.; Zhang, Z.; Wang, F.; Wei, W.; and Xu, Y. 2022a. Spatial-Temporal Identity: A Simple yet Effective Baseline for Multivariate Time Series Forecasting. In *Proceedings of the 31st ACM International Conference on Information & Knowledge Management*, 4454–4458.
- Shao, Z.; Zhang, Z.; Wei, W.; Wang, F.; Xu, Y.; Cao, X.; and Jensen, C. S. 2022b. Decoupled dynamic spatial-temporal graph neural network for traffic forecasting. *arXiv preprint arXiv:2206.09112*.
- Srinivasan, B.; and Ribeiro, B. 2019. On the equivalence between positional node embeddings and structural graph representations. *arXiv preprint arXiv:1910.00452*.
- Ulyanov, D.; Vedaldi, A.; and Lempitsky, V. 2016. Instance normalization: The missing ingredient for fast stylization. *arXiv preprint arXiv:1607.08022*.
- Vaswani, A.; Shazeer, N.; Parmar, N.; Uszkoreit, J.; Jones, L.; Gomez, A. N.; Kaiser, Ł.; and Polosukhin, I. 2017. Attention is all you need. In *Advances in neural information processing systems*, 5998–6008.
- Wu, F.; Souza, A.; Zhang, T.; Fifty, C.; Yu, T.; and Weinberger, K. 2019a. Simplifying graph convolutional networks. In *International conference on machine learning*, 6861–6871. PMLR.
- Wu, H.; Hu, T.; Liu, Y.; Zhou, H.; Wang, J.; and Long, M. 2022. TimesNet: Temporal 2D-Variation Modeling for General Time Series Analysis. *arXiv preprint arXiv:2210.02186*.
- Wu, H.; Xu, J.; Wang, J.; and Long, M. 2021. Autoformer: Decomposition transformers with auto-correlation for long-term series forecasting. *Advances in Neural Information Processing Systems*, 34: 22419–22430.
- Wu, Z.; Pan, S.; Long, G.; Jiang, J.; Chang, X.; and Zhang, C. 2020. Connecting the Dots: Multivariate Time Series Forecasting with Graph Neural Networks. In *Proceedings of the 26th ACM SIGKDD International Conference on Knowledge Discovery and Data Mining*, 753–763. New York, NY, USA: Association for Computing Machinery.
- Wu, Z.; Pan, S.; Long, G.; Jiang, J.; and Zhang, C. 2019b. Graph Wavenet for Deep Spatial-Temporal Graph Modeling. In *Proceedings of the 28th International Joint Conference on Artificial Intelligence*, 1907–1913.
- Xu, M.; Dai, W.; Liu, C.; Gao, X.; Lin, W.; Qi, G.-J.; and Xiong, H. 2020. Spatial-temporal transformer networks for traffic flow forecasting. *arXiv preprint arXiv:2001.02908*.
- Yang, C.; Wu, Q.; Wang, J.; and Yan, J. 2022. Graph Neural Networks are Inherently Good Generalizers: Insights by Bridging GNNs and MLPs. *arXiv preprint arXiv:2212.09034*.
- Yu, B.; Yin, H.; and Zhu, Z. 2018. Spatio-temporal graph convolutional networks: a deep learning framework for traffic forecasting. In *Proceedings of the 27th International Joint Conference on Artificial Intelligence*, 3634–3640.
- Zeng, A.; Chen, M.; Zhang, L.; and Xu, Q. 2022. Are transformers effective for time series forecasting? *arXiv preprint arXiv:2205.13504*.
- Zhang, Q.; Chang, J.; Meng, G.; Xiang, S.; and Pan, C. 2020. Spatio-temporal graph structure learning for traffic forecasting. In *Proceedings of the AAAI conference on artificial intelligence*, volume 34, 1177–1185.
- Zhang, T.; Zhang, Y.; Cao, W.; Bian, J.; Yi, X.; Zheng, S.; and Li, J. 2022. Less is more: Fast multivariate time series forecasting with light sampling-oriented mlp structures. *arXiv preprint arXiv:2207.01186*.
- Zheng, C.; Fan, X.; Wang, C.; and Qi, J. 2020. Gman: A graph multi-attention network for traffic prediction. In *Proceedings of the AAAI Conference on Artificial Intelligence*, volume 34, 1234–1241.
- Zheng, Y.; Yi, X.; Li, M.; Li, R.; Shan, Z.; Chang, E.; and Li, T. 2015. Forecasting fine-grained air quality based on big data. In *Proceedings of the 21th ACM SIGKDD international conference on knowledge discovery and data mining*, 2267–2276.

Appendix

A Detailed Experimental Settings

A.1 Dataset Descriptions

We adopt several public traffic flow datasets to benchmark our model. All of them are medium-sized datasets and are widely used in relevant studies. Statistics information is provided in Tab. 5.

Table 5: Statistics of datasets used in the experiments.

DATASETS	Type	Steps	# of Nodes	# of Edges	Windows
METR-LA	speed	34,272	207	1515	5 min
PEMS-BAY	speed	52,128	325	2369	5 min
PEMS03	volume	26,208	358	546	5 min
PEMS04	volume	16,992	307	340	5 min
PEMS07	volume	28,224	883	866	5 min
PEMS08	volume	17,856	170	277	5 min
TrafficL	occupancy	17544	862	-	60 min

Traffic Speed Datasets Our experiments include two commonly used traffic speed datasets, named METR-LA and PEMS-BAY. METR-LA contains spot speed data from 207 loop sensors over a period of 4 months from Mar 2012 to Jun 2012, located at the Los Angeles County highway network. PEMS-BAY records 6 months of speed data from 325 static detectors in the San Francisco South Bay Area.

Traffic Volume Datasets There are four traffic volume datasets to evaluate our model, including PEMS03, PEMS04, PEMS07, and PEMS08. PEMS0X contains the real-time highway traffic volume information in California, which is collected by the Caltrans Performance Measurement System (PeMS) (Chen et al. 2001) in every 30 seconds. The raw traffic flow data is aggregated into 5-minute interval for experiments. Similar to METR-LA and PEMS-BAY, PEMS0X also includes a sensor graph calculated by the physical distance between sensors.

Traffic Occupancy Datasets TrafficL is a common benchmark for the LTSF task. This data is a collection of 48-month (2015-2016) hourly measurements from the PeMS, which describes the road occupancy rates (between 0 and 1). Note that TrafficL does not provide an adjacent matrix.

A.2 Baseline Methods

We select several widely discussed baseline models in the time series forecasting literature. All the adopted baseline models are described as follows:

1. **STCN**: spectral graph convolution networks combined with 1-D temporal convolutions (Yu, Yin, and Zhu 2018);
2. **DCRNN**: diffusion convolutional recurrent neural network, which is a typical baseline in traffic forecasting (Li et al. 2018);
3. **GWNet**: this model alternates graph convolution and 1-D dilated convolution with given and learned graphs (Wu et al. 2019b);

4. **AGCRN**: graph convolution recurrent networks with adaptively learned graphs (Bai et al. 2020);
5. **ST-Transformer**: spatial-temporal Transformer model with self-attention computations on both space and time dimensions (Xu et al. 2020);
6. **MTGNN**: advanced graph learning module with a WaveNet backbone (Wu et al. 2020);
7. **EvolveGCN**: GCN along the temporal dimension to capture the dynamism of the graph sequence and RNNs are used to evolve the GCN parameters (Pareja et al. 2020);
8. **STID**: simple MLP model with spatial and temporal identifications, which achieve comparable performances on several benchmarks (Shao et al. 2022a);
9. **GatedGN**: a state-of-the-art time-then-graph model where a gated attention mechanism is used over the whole graph to perform spatial aggregation and convolution (Satorras, Rangapuram, and Januschowski 2022);
10. **D2STGNN**: this model decoupled traffic signal into diffusion parts and inherent parts, and a dynamic graph learning module is also introduced (Shao et al. 2022b);
11. **DLinear**: simple linear models (Zeng et al. 2022) with time series decomposition (Wu et al. 2021) for long-term time series forecasting;
12. **TimesNet**: state-of-the-art general time series model with 2-D periodicity representations, which adopts the inception block as backbones (Wu et al. 2022);
13. **SCINet**: SCINet is a recursive downsample-convolve-interact architecture which models temporal correlation with sample convolutions (Liu et al. 2022);
14. **GRUGCN**: time-then-graph model with a GRU encoder and a GCN decoder structure (Gao and Ribeiro 2022);
15. **DGCRN**: state-of-the-art graph convolution recurrent architecture that constructs dynamic graph at each time step (Li et al. 2023).

A.3 Experimental Setup

Short-term Traffic Benchmarks For short-term datasets, we adopt the same training (70%), validating (10%), and testing (20%) set splits and preprocessing steps as (Wu et al. 2019b). All six short-term benchmarks provide the adjacent matrix \mathbf{A} based on the Gaussian kernel, which is worth commenting that NexuSQN does not rely on \mathbf{A} , and results in Tab. 4 indicate that the benefits of incorporating predefined graphs are marginal. Time-of-day information is provided as exogenous variables for our model, and day-of-week feature is input to baselines that require this information. In addition, labels with nonzero values are used to compute the metrics. And the performance of all methods is recorded in the same testing environment.

Long-term Traffic Benchmarks We adopt the experimental setup in (Wu et al. 2022), where the pase sequence length is set to 96 and predictions at the next {96,192,288,384} steps are used to calculate the metrics. Slightly different, here we do not use the standardization on labels and use the normalized mean absolute error (NMAE), mean relative error (MRE), and mean absolute percentage error (MAPE) as metrics.

Ablation Study We consider the following three variations of NexuSQN:

- w \mathbf{A}_{pre} : We add additional diffusion graph convolutions (Li et al. 2018) with three forward and backward diffusion steps using distance-based graphs in SpaceMixer and combine it with dense graphs \mathbf{A}_t .
- w \mathbf{S}_{emb} : We replace the “when locator” design by using timestamp embeddings at each step. In this scenario, our model shares a structure similar to that of STID (Shao et al. 2022a).
- w/o \mathbf{E} : We remove the “where” and “when” locators, and our model degrades into a spatial-temporal MLP mixer in Eq. 5.

For each of them, we keep the same experimental settings in section 5 and report the forecasting results.

B Reproducibility

Platform All these experiments are conducted on a Windows platform with one NVIDIA RTX 3080 GPU. The maximum GPU memory resource is 10 GB. Our implementations are mainly rely on PyTorch (Paszke et al. 2019) and Torch Spatiotemporal² (Cini and Marisca 2022). The realization of baseline models and hyperparameter settings are also based on BasicTS³. Our code to reproduce the reported results will be open-sourced upon publication.

Hyperparameters Our NexuSQN contains only a few model hyperparameters and is easy to tune. The detailed configurations of all datasets are shown in Tab. 6. The configurations of other baseline models and implementations follow the official resources as much as possible.

Model configurations		PEMS03	PEMS04	PEMS07	PEMS08
Hyperparameter	hidden_size	128			
	mp_layers	2	2	2	1
	activation	SiLU			
	st_embed	False	True	True	False
	layer_res	True			
Training configs	window_size	12			
	horizon	12			
	batch_size	32			
	learning_rate	0.005			
	lr_gamma	0.1			
	lr_milestones	[40,60]			
Model configurations		METR-LA	PEMS-BAY	TrafficL	
Hyperparameter	hidden_size	64	64	64	
	mp_layers	2	2	3	
	activation	SiLU			
	st_embed	False	False	True	
	layer_res	False			
Training configs	window_size	12			
	horizon	12			
	batch_size	64	64	32	
	learning_rate	0.005			
	lr_gamma	0.1			
	lr_milestones	[20,30,40]			

Table 6: Hyperparameters of NexuSQN

Pseudo Codes We provide a concise implementation of NexuSQN following the PyTorch format in Algorithm 1.

²<https://github.com/TorchSpatiotemporal/tsl>

³<https://github.com/zezhihao/BasicTS>

Algorithm 1: Pseudo Code for Forward of NexuSQN

```

# linear: fully-connected layers
# ins: instance normalization layers
# fold/unfold: tensor flattening/unflattening layers
# silu: activation function
# x: input data sized [B, T, N, D], B for batch size, T
    for window size, N for node numbers, D for channels
# e: spatiotemporal node embedding

def forward(x):
    # input flattening and projection
    x = fold(x)
    x = silu(linear(x))
    # time mixing
    x = x + e # where locator
    x_res = x
    x = silu(linear(x))
    x = ins(x)
    x = x + linear(x_res)
    # space mixing
    A = softmax(bmm(e,e.T),dim=-1)
    for i in enumerate(mp_layers):
        x = x + e # where locator
        x_res = x
        x = linear(x)
        x = bmm(A,x) # message-passing as when locator
        x = silu(x)
        x = ins(x)
        x = x + x_res
    # dense readout
    x = silu(linear(x))
    y_pred = unfold(linear(x))
    return y_pred

```

C Additional Discussions and Interpretations

C.1 Model Architecture Details

Positional Encoding We adopt sinusoidal PE to inject the time-of-day information of each time series along time dimension:

$$\begin{aligned}
 PE_{\text{sine}} &= \sin(p_i * 2\pi / \delta_D), \\
 PE_{\text{cosine}} &= \cos(p_i * 2\pi / \delta_D), \\
 \mathbf{U}_t &= [PE_{\text{sine}} || PE_{\text{cosine}}],
 \end{aligned} \tag{14}$$

where p_i is the index of i -th time point in the series, and δ_D is the day-unit time mapping. We concatenate PE_{sine} and PE_{cosine} as the final temporal encoding. In fact, day-of-week embedding can also be applied using the one-hot encoding.

Node Embedding Node embedding can be implemented by initializing a parameter with its gradient trackable:

```

self.emb = nn.Parameter(
    Tensor(self.num_nodes, self.emb_size),
    requires_grad=True)

```

The initialization method (e.g., Gaussian or uniform distribution) can be used to specify its initial distribution.

Residual Connection We have attempted two types of residual connection in the TimeMixer, which we call them *layer-wise* and *block-wise* residual connections. Specifically speaking, *layer-wise* residual connection indicates that there exists a global skip connection that linearly maps the look-back series to a hidden state. While in *block-wise* setting

we use a skip connection per operation. Such designs ensure `TimeMixer` can embody a class of linear models like (Zeng et al. 2022; Chen et al. 2023).

Normalization We adopt the instance normalization (Ulyanov, Vedaldi, and Lempitsky 2016) to reinforce the representations of local components:

$$\tilde{h}_i^t = \frac{h_i^t - \mathbb{E}[h_i^t]}{\sqrt{\text{Var}[h_i^t] + \epsilon}} \gamma_i + \beta_i, \quad (15)$$

where γ and β are learnable parameters, and the expectation and variance are calculated per-dimension separately for each item in a mini-batch. Eq. 15 is equivalent to the temporal normalization (Deng et al. 2021), so that the encoder can better exploit high-frequency representations. As discussed in (Kim et al. 2021), when the distribution shifts between training and testing, a reversible IN can be utilized.

Parameter-efficient Neural Message Passing There are two technical key points in this parameter-efficient design:

1. Dense graph with fewer layers: we use small number of dense graph aggregations (e.g., 2 layers in most cases) to capture large spatial receptive field;
2. Shared mixing layer: the `linear` operator is shared between consecutive MP layers to mix the time dimensions.

A crucial aspect to consider when utilizing a dense relation graph is that it prompts the model to gather comprehensive information from other series in order to obtain a precise “when locator”. And the parameter sharing design may shed light on the connection between MLPs and GNNs.

C.2 Relationships with Related Works

In this detailed section on related work, we highlight recent advances in simplified neural forecasting models. Our objective is to establish a nexus between notable breakthroughs by offering a meticulous exposition on two primary research avenues: (1) simplistic models for LTSF; and (2) node embedding in STGNNs, the unification of which served as the catalyst for driving the development of this work.

Simplistic Models for LTSF Within the literature on time series studies, LTSF is considered one of the most challenging tasks. Encouragingly, recent studies have revisited neural architecture design and seek a simpler solution for this long-standing topic and empirically show the superiority of small models over their complex counterparts (Zeng et al. 2022; Zhang et al. 2022; Das et al. 2023; Chen et al. 2023). In particular, Zeng et al. (2022) analyze the ineffectiveness of Transformer-based models on this task and outperform an array of advanced baselines with a family of linear models. Chen et al. (2023) develop a fully MLP model that performs mixing operations along both the time and the feature dimensions, called TSMixer. The cross-sensor information is utilized by a weighted sum of all series. TiDE proposed by (Das et al. 2023) enjoys a dense encoder-decoder structure with a residual MLP backbone. The channel-independence design in DLinear (Zeng et al. 2022), TiDE (Das et al. 2023) and PatchTST (Nie et al. 2022) makes the model a global univariate one. While the channel mixing in (Chen et al.

2023; Zhang et al. 2022) implicitly models the relationships between series.

However, investigation into short-term spatiotemporal forecasting problem is still lacking. Different from LTSF, the studied STTF is more challenging in two ways: (1) more complex temporal patterns (e.g., nonstationary) with high resolution; (2) subtle interaction between different series (locations). Therefore, we conjecture that the emerging Transformers-like or MLP-based models designed for LTSF are less effective in the context of spatiotemporal data, as the above methods basically adopt a channel-independence assumption and ignore the explicit correlations between series (Zeng et al. 2022; Das et al. 2023).

Node Embedding in STGNNs Node embedding or positional encoding in the graph machine learning domain is a commonly used technique to enhance the expressive power of GNNs (Dwivedi et al. 2022). While, methodologies and applications on spatiotemporal graph modeling have been relatively limited.

In this line of research, Deng et al. (2021) identify the bottleneck of deep forecasting models as ineffectiveness in distinguishing high-frequency components from input signals. A spatial-temporal normalization scheme is proposed to enhance the WaveNet models. Shao et al. (2022a) discuss the spatial-temporal identification problem and propose to assign a learnable embedding for each node and time step. GatedGN model proposed in (Satorras, Rangapuram, and Januschowski 2022) follows a time-then-graph template and considers the node index as a static identifier. Global attention is used to infer the latent graphs. However, all pairwise attention with time complexity $\mathcal{O}(n^2)$ is computationally very expensive. Most recently, Cini et al. (2023) interpret the role of node embedding as local effects in global models and provide a systematic framework to incorporate it into different architectures.

Building upon the existing works, our research resides at the crossroads of these two research trajectories. To the best of our knowledge, we are among the first to develop a skillful and integrated neural architecture for multivariate time series modeling that directly expresses spatial-temporal contextualization with essentially connected components, and demonstrate performance that rivals state-of-the-art results with much higher computational efficiency.

D Supplementary Results

This section provides additional results on the forecasting performance of NexuSQN. In addition to traffic data, NexuSQN has the potential to model and analyze general multivariate time series from other domains. We perform evaluations on two additional datasets, including AQI (Zheng et al. 2015) and PV-US (Hummon et al. 2012):

- AQI data records PM2.5 pollutant measurements collected by 437 air quality monitoring stations across 43 Chinese cities from May 2014 to April 2015 with the aggregation interval being 1 hour. Note that AQI contains nearly 26% missing data;
- Large-scale PV-US production data consists of a simulated energy production by 5016 PV farms in United

	AQI				PV-US			
	1 h	2 h	3 h	Ave.	0.5 h	7.5 h	11 h	Ave.
	MAE	MAE	MAE	MAE	MAE	MAE	MAE	MAE
AGCRN	10.78	14.32	16.96	14.02	-	-	-	-
DCRNN	9.89	13.79	16.78	13.49	1.65	2.94	3.16	2.79
GWNNet	9.39	12.98	15.71	12.70	1.48	6.13	7.66	4.86
GatedGN	10.39	14.68	17.76	14.28	1.61	3.23	3.06	2.74
GRUGCN	10.02	13.95	16.92	13.63	1.44	2.89	2.96	2.62
EvolveGCN	10.64	15.02	18.27	14.64	-	-	-	-
ST-Transformer	10.13	14.17	17.01	13.77	-	-	-	-
STCN	9.63	13.47	16.47	13.19	1.88	6.83	7.68	5.47
STID	10.44	14.76	17.88	14.36	1.42	2.67	2.76	2.45
MTGNN	10.24	14.10	16.83	13.72	1.81	3.11	3.14	2.96
D2STGNN	9.48	12.91	15.44	12.61	-	-	-	-
DGCRN	-	-	-	-	-	-	-	-
DLinear	10.99	15.79	19.31	15.36	1.59	3.11	3.08	3.27
TimesNet	17.64	19.47	21.10	19.40	1.47	2.75	2.80	2.51
NexuSQN	9.45	12.90	15.45	12.60	1.26	2.65	2.69	2.33

Table 7: Results on AQI and PV-US benchmarks. Note that - indicates the model runs out of memory with the minimum batch size. Best results are bold marked.

States during 2006. The original observations are aggregated into a 30-min window.

For AQI, we set the size of the input window as 24 steps (24 hours) and forecasting horizon as 3 steps (3 hours). While for large-scale energy data, we adopt the settings in (Cini et al. 2022) that 36-steps are used as inputs and predictions at next {00 : 30, 07 : 30, 11 : 00} hours are used for evaluation.

Results in Tab. 7 indicate great potentials of NexuSQN to handle time series with insignificant spatial relations and large spatial dimensions.